Stellar Atmosphere Modeling
ASP Conference Series, Vol. 288, 2003
I. Hubeny, D. Mihalas, & K. Werner, eds.

Numerical Solutions of Polarized Line Transfer Equations

K.N. Nagendra

Indian Institute of Astrophysics, Bangalore 560 034, India

Abstract. Developments in the NLTE polarized line transfer theory are reviewed. Attention is focused on theoretical aspects of the problem. Basic ideas of an exact (or direct) method called 'Discrete Space Method' (DSM) are presented, with two applications – namely the non-magnetic resonance scattering polarization in spherically symmetric media, followed by polarized line formation in moving media. Secondly, the essential steps of 'Polarized Approximate Lambda Iteration' (PALI) method for Hanle effect with CRD and PRD line scattering, are briefly described. The performance of these methods is illustrated through a study of iterative convergence. Advantages of PALI methods over direct methods are highlighted.

1. Introduction

The resonance scattering in a spectral line produces linearly polarized radiation (Hamilton 1947). This non-magnetic dipole scattering involving the bound levels of an atom is equivalent to the Rayleigh scattering on molecules. The relevant scattering phase matrix in the Stokes vector $(\mathrm{I\ Q\ U\ V})^{\mathrm{T}}$ representation was derived by Chandrasekhar (1950), who also solved the concerned 'monochromatic' polarized radiative transfer problem exactly. We give below a brief historical perspective on the methods to solve polarized line transfer problems. An assumption of axial symmetry allows to work with transfer equation for the restricted Stokes vector $(\mathrm{I\ Q})^{\mathrm{T}}$. Such an equation represents a generalization of the scalar NLTE equations, to include linear polarization in spectral lines.

The work of Stenflo & Stenholm (1976), assuming Stokes-Q as a perturbation, under Rybicki's core saturation method (for CRD), represents the earliest solution of polarized line transfer equation. The polarized integral equation methods assuming CRD (Rees 1978), and the PRD (Mc Kenna 1984); the differential equation methods such as the Feautrier method for PRD with Stokes-Q treated as a perturbation (Rees & Saliba 1982), non-perturbative Feautrier method with PRD (Dumont et al. 1977; Faurobert 1987); the non-iterative, non-perturbative DSM with PRD (Nagendra 1986, 1988) represent some of the 'exact numerical methods' for solving this problem. They require greater computer memory and are slow compared to the 'Approximate Lambda Iteration' (ALI) approach (based on the operator splitting). A review of analytic/asymptotic methods in polarized line transfer is presented by Ivanov et al. (1991).

The PALI methods were developed in the 1990's. The progress here has taken place in two parallel streams - the stream-1 is based on the 'atomic den-

sity matrix formalism' of polarized line transfer, developed by Bommier & Sahal-Brechot (1978), and Landi Degl' Innocenti (1982, 1983, 1984, 1985). The stream-2 is based on the 'scattering phase matrix formalism' (presented in: Mihalas 1978; Rees 1978; Stenflo 1994; Ivanov 1997). Each stream has its own advantages and limitations. However both the streams have followed 'scalar ALI method' developed by Olson, Auer, & Buchler (1986). A fine review about unpolarized ALI methods is written by Hubeny (1992). The applications of PALI method to the stream-1 are presented in Trujillo-Bueno & Landi Degl'Innocenti (1996, 1997), and Trujillo-Bueno & Manso Sainz (1999). Similar applications to the stream-2 are presented in Rees & Murphy (1987), Faurobert, Frisch, & Nagendra (1997), and Paletou & Faurobert (1997). These PALI methods developed initially for prototype non-magnetic resonance scattering problem, were later generalized to the case of Hanle effect, independently under both the streams. Hanle effect is essentially a modification of resonance scattering polarization, by a weak magnetic field. The PALI method using stream-1 is presented in Manso Sainz & Trujillo-Bueno (1999), later extended in Manso Sainz & Trujillo-Bueno (2001). Generalization of PALI in stream-2, is presented in Nagendra, Frisch, & Faurobert (1998, CRD with Hanle effect), Nagendra et al. (1999, PRD with Hanle effect), and Fluri, Nagendra, & Frisch (2002, exact collisional PRD with Hanle effect). See Frisch (1998, 1999) for a discussion on the equivalence of stream-1 and stream-2.

2. The Basic Equations of Polarized Line Transfer in Axi-symmetry

The polarized 2-level atom line radiative transfer equation (RTE) is given by

$$\mu \frac{\partial \boldsymbol{\mathcal{I}}(\tau, x, \mathbf{n})}{\partial \tau} = [\phi(\tau, x) + \beta(\tau)] \, [\boldsymbol{\mathcal{I}}(\tau, x, \mathbf{n}) - \boldsymbol{\mathcal{S}}(\tau, x, \mathbf{n})] \,, \tag{1}$$

in the usual notation (see Mihalas 1978). $\boldsymbol{\mathcal{I}} = (\mathrm{I}\ \mathrm{Q})^{\mathrm{T}}$ is the Stokes intensity vector, and $\boldsymbol{\mathcal{S}}$ is the Stokes source vector. ϕ is profile function, and $\beta = k^C/k^L$ the continuum absorption parameter. The total source vector is given by

$$\boldsymbol{\mathcal{S}}(\tau, x, \mathbf{n}) = \frac{\phi(\tau, x) \, \boldsymbol{\mathcal{S}}_\ell(\tau, x, \mathbf{n}) + \beta(\tau) \, \boldsymbol{\mathcal{S}}_\mathbf{c}(\tau)}{\phi(\tau, x) + \beta(\tau)} \,. \tag{2}$$

The continuum source vector (assumed here as unpolarized) is given by $\boldsymbol{\mathcal{S}}_\mathbf{c} = B_{\nu_o}(\tau) \, \boldsymbol{\mathcal{U}}$; where $\boldsymbol{\mathcal{U}} = (1 \ \ 0)^T$. The polarized line source vector is written as

$$\boldsymbol{\mathcal{S}}_\ell(\tau, x, \mathbf{n}) = \varepsilon B_{\nu_o} \, \boldsymbol{\mathcal{U}} + \frac{(1-\varepsilon)}{\phi(\tau, x)} \int_{-\infty}^{+\infty} dx' \oint \frac{d\Omega'}{4\pi} R(\tau, x, x') \, \hat{P}(\mathbf{n}, \mathbf{n}') \, \boldsymbol{\mathcal{I}}(\tau, x', \mathbf{n}') \,. \tag{3}$$

In the above equation, we have employed the "factorization of frequencies & angles" - which means: redistribution matrix $\simeq$ redistribution function $*$ phase matrix. The most basic frequency redistribution function $R(x, x')$ that can be used in Eq. (3) is CRD – which is a reasonable assumption for scattering in weak lines; $[R_{\mathrm{II}}, R_{\mathrm{III}}]$ combination – which is good approximation for resonance

lines, and $[R_{\rm V}, R_{\rm III}]$ combination – which is applicable for subordinate lines. The functions R_i, $i = {\rm I, II, III}$, and V are derived by Hummer (1962), and Heinzel (1981) respectively. The phase matrices required for polarized transfer are presented in Chandrasekhar (1950), and Stenflo (1994). The (2 x 2) axially-symmetric part of the Rayleigh phase matrix is given by

$$\hat{P}(\mu,\mu') = \hat{E}_{11} \; + \; \frac{3}{4}\hat{P}_0^2(\mu,\mu'), \tag{4}$$

which is a weighted sum of 'isotropic scattering phase matrix', and the 'dipole scattering phase matrix' written explicitly as

$$\hat{P}(\mu,\mu') = \begin{pmatrix} 1 & 0 \\ 0 & 0 \end{pmatrix} + \frac{3}{8}\begin{pmatrix} \frac{1}{3}(1-3\mu^2)(1-3\mu'^2) & (1-3\mu^2)(1-\mu'^2) \\ (1-\mu^2)(1-3\mu'^2) & 3(1-\mu^2)(1-\mu'^2) \end{pmatrix}. \tag{5}$$

The above five equations define the prototype polarized line transfer problem. The "factorization" is an ad-hoc assumption, but substantially simplifies the line transfer computations. The use of angle dependent redistribution function $R(x,x',\Theta)$ is a better choice instead of the angle averaged function $R(x,x')$.

3. A Brief Discussion of the Discrete Space method (DSM)

There are two classes of direct methods namely (1) coupled integral equation methods for $({\rm I\ Q})^{\rm T}$ and (2) coupled differential equation methods for $({\rm I\ Q})^{\rm T}$. The DSM is a finite difference, discrete ordinate method based on first order form of the transfer equation. We describe below the essential ideas underlying this method. Basically we divide the medium into N-layers of arbitrary optical thickness. Our purpose is to compute the reflection (r) and transmission (t) operators for each layer, the construction of which is based on the concept of "linear interaction principle". For the sake of brevity, and extension of scalar equations to the polarized case we use the notation

$$I^{\pm} = \begin{pmatrix} {\rm I}^{\pm} \\ {\rm Q}^{\pm} \end{pmatrix}; \quad \Sigma^{\pm} = \begin{pmatrix} \Sigma_{\rm I}^{\pm} \\ 0 \end{pmatrix}; \quad t = \begin{pmatrix} t_{\rm I} & 0 \\ 0 & t_{\rm Q} \end{pmatrix}; \quad r = \begin{pmatrix} r_{\rm I} & 0 \\ 0 & r_{\rm Q} \end{pmatrix} \quad \text{etc.} \tag{6}$$

Linear Interaction Principle:
It is a statement of the relation between 'incident' and 'outgoing' radiation field, for a layer of given thickness. Consider a layer bounded by the planes n and $n+1$ (see Fig. (1a)). Let column vectors $I_n^{\pm} = [I_n(\pm\mu_1), I_n(\pm\mu_2), ...I_n(\pm\mu_J)]$ for incoming rays $(+\mu)$ and outgoing rays $(-\mu)$ be discrete representation of intensity I on a μ - grid $(0 < \mu_j < 1)$, $j = 1, 2, ..., J$. Let the column vectors $\Sigma_{n+1,n}^{+}$ and $\Sigma_{n,n+1}^{-}$ represent the contribution from internal sources of radiation. If we assume that response of the layer is linear to the incident radiation, then we can write the "interaction principle" as

$$\begin{pmatrix} I_{n+1}^{+} \\ I_n^{-} \end{pmatrix} = \begin{pmatrix} t(n+1,n) & r(n,n+1) \\ r(n+1,n) & t(n,n+1) \end{pmatrix} \begin{pmatrix} I_n^{+} \\ I_{n+1}^{-} \end{pmatrix} + \begin{pmatrix} \Sigma_{n+1,n}^{+} \\ \Sigma_{n,n+1}^{-} \end{pmatrix}, \tag{7}$$

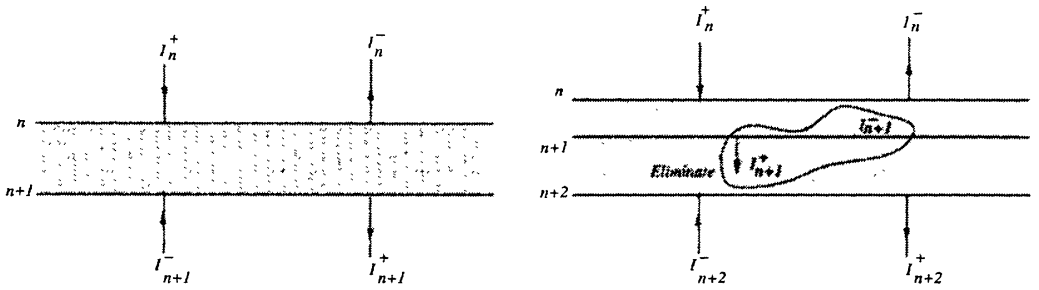

Figure 1. (**a**: Left) The linear interaction principle for a single layer. (**b**: Right) Combined response of two arbitrary layers placed adjacently.

or when expressed in terms of the interaction matrix $S(n, n+1)$ and the internal source matrix $\Sigma(n, n+1)$, we can write

$$\begin{pmatrix} I_{n+1}^+ \\ \\ I_n^- \end{pmatrix} = S(n, n+1) \begin{pmatrix} I_n^+ \\ \\ I_{n+1}^- \end{pmatrix} + \Sigma(n, n+1) \; . \tag{8}$$

Interaction Principle for a Composite Layer:
Consider another layer bounded by the planes $n+1$ and $n+2$. The linear response of this layer, considered independently is

$$\begin{pmatrix} I_{n+2}^+ \\ \\ I_{n+1}^- \end{pmatrix} = S(n+1, n+2) \begin{pmatrix} I_{n+1}^+ \\ \\ I_{n+2}^- \end{pmatrix} + \Sigma(n+1, n+2). \tag{9}$$

We intend to calculate the combined response of both the layers when placed together, as shown in Fig. (1b). The 'interaction principle' for the layer $(n, n+2)$ can be written directly as

$$\begin{pmatrix} I_{n+2}^+ \\ \\ I_n^- \end{pmatrix} = S(n, n+2) \begin{pmatrix} I_n^+ \\ \\ I_{n+2}^- \end{pmatrix} + \Sigma(n, n+2). \tag{10}$$

What is important is that we can also obtain the matrix $S(n, n+2)$ in terms of $S(n, n+1)$ and $S(n+1, n+2)$. The product $S(n, n+2) = S(n, n+1) * S(n+1, n+2)$ is called the "star product", and simply involves elimination of I_{n+1}^+ and I_{n+1}^- at the common interface $(n+1)$. The 'elimination process' leads to the relevant expressions for the r and t operators of the 'composite layer'. The r and t operator were originally derived by Redheffer (1962). The internal source operators were later incorporated by Grant & Hunt (1969a,b). The definition and construction of unpolarized r, t and Σ operators in terms of the physical variables is described in Peraiah (2001). The integration of the transfer equation over a computational cell, and finite difference discretization, are explained in the same reference. The corresponding equations for polarized line transfer are described in Nagendra (1986, 1988, 1994). For lack of space here, the full details are presented as extended notes, and placed at the author's web site, which may be accessed at `http://www.iiap.ernet.in/nagendra/nagendra-dsm.ps`.

4. Two Sample Results by the DSM Method

In this Section we present two results computed by the DSM.

4.1. Polarized Line Transfer in a Static Spherical Media

In a well known review article, Hubeny (1985) mentioned several "non-standard problems" in stellar spectral line formation theory. The 'polarized resonance scattering line transfer in static/moving spherical Media' was one such example. The problem was subsequently solved in Nagendra (1988) for static spherical media (with PRD), and in Jeffery (1989, 1990) for 'moving spherical media' by Sobolev-P method applied to spherical winds (with CRD). Polarized line transfer equation in spherical geometry is written as:

$$\mu \frac{\partial \boldsymbol{\mathcal{I}}(r,x,\mathbf{n})}{\partial r} + \frac{1-\mu^2}{r}\frac{\partial \boldsymbol{\mathcal{I}}(r,x,\mathbf{n})}{\partial \mu} = k^L(r)\left[\phi(r,x)+\beta(r)\right]\left[-\boldsymbol{\mathcal{I}}(r,x,\mathbf{n})+\boldsymbol{\mathcal{S}}(r,x,\mathbf{n})\right], \quad (11)$$

where, $\boldsymbol{\mathcal{I}} = (\mathrm{I}\ \mathrm{Q})^{\mathrm{T}}$; and $\boldsymbol{\mathcal{S}} = (S_{\mathrm{I}}\ S_{\mathrm{Q}})^{\mathrm{T}}$ are the Stokes intensity and total source vectors. To compute Fig. (2a) we employ the following model parameters: Total optical depth $T^L = 10^6$; Damping parameter $a = a_{\mathrm{u}} + a_{\mathrm{l}} = 10^{-2}$; Thermalization parameter $\varepsilon = 10^{-4}$; Continuous absorption coefficient $k^C(r) = \beta k^L(r)$, with $\beta = \beta^C = 10^{-4}$; Line absorption coefficient $k^L(r) = Kr^{-2}$, with $K = RT^L/(R-1)$; Line optical depth scale $\tau^L(r) = K[(R-r)/rR]$; Inner radius of the spherical shell $R_c = 1$; Internal thermal source $B(r) = 1$ ie., an isothermal spherical shell, with a photon creation rate per unit optical depth proportional to r^2; Inner boundary condition $\boldsymbol{\mathcal{I}}(R_c,x,\mu) = (B_{\nu_o}\ 0)^{\mathrm{T}}$; Outer boundary condition $\boldsymbol{\mathcal{I}}(R,x,-\mu) = 0$; PRD function $R(x,x') = (2/3)R_{\mathrm{V-AA}}(x,x') + (1/3)R_{\mathrm{III-AA}}(x,x')$, to represent collisional effects in a subordinate line (Heinzel 1981; Nagendra 1988). Results are shown for $R = 1$ (case 1, planar slab), and $R = 3, 9, 27, 81, 122, 162, 203,$ and 243 (cases 2-9, spherically symmetric media).

Fig. (2a) shows intensity $\mathrm{I}(x,\mu)$ and polarization profiles $p = \mathrm{Q}(x,\mu)/\mathrm{I}(x,\mu)$ at $\mu = 0.11$. The frequency (x) scale on top of Fig. (2a) refers to these line profiles. The lower two sets of curves show source functions S_{I} and S_{Q}, plotted as a function of optical depth τ. Sharp peak in S_{Q} for the planar case ($R = 1$) can be explained through frequency thermalization effects. The influence of spherical dilution is seen in the τ-dependence of S_{I}. Recall that sphericity of the medium affects line polarization through (1) bias in scattering preferentially toward larger radii; (2) spherical dilution of radiation field; and (3) outward peaking of radiation field toward radial directions (see Mihalas 1978).

The main conclusions from Fig. (2a) are: (1) the formation of near wing negative polarization peaks can be explained in terms of spherical dilution; (2) emergent intensity decreases by rather small factor of 20 when R changes from 1 to 243 because of strong continuous absorption. (3) peaking of radiation at large radii is partly responsible for mid-wing polarization peaks. (4) PRD effects are stronger in spherical media, compared to planar media, due to larger angular anisotropy in the former case. (5) Sphericity effects are stronger in PRD case, compared to the CRD case, because of 'partially coherent nature' of $R_{\mathrm{V-AA}}(x,x')$ in the line wings, leading to an increased role of multiple scattering within the atmosphere. (6) nature of anisotropy is different in planar

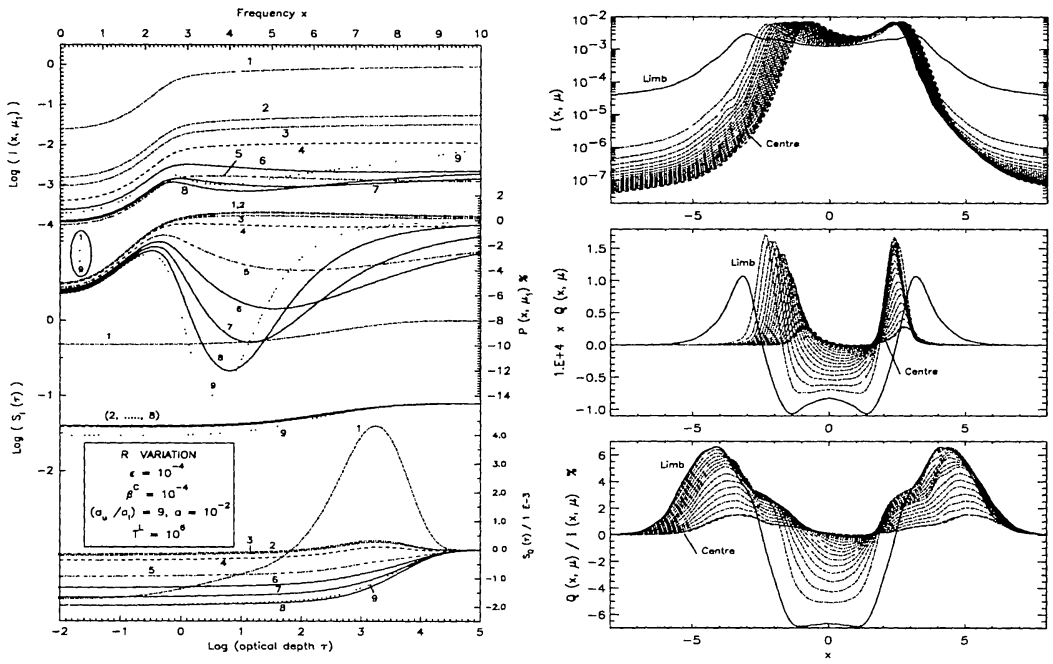

Figure 2. (**a**: Left) Polarization of radiation emitted by extended spherical atmospheres (extension R is free parameter). (**b**: Right) Polarization of emission lines formed in a moving planar atmosphere.

and extended ($R \gg 10$) spherical atmospheres. See Nagendra (1995) for more details.

4.2. Polarized Line Transfer in Moving Media by CMF Method

There are two approaches of solving this problem, namely the rest frame method (RFM), and the co-moving frame (CMF) method. See Mihalas (1978) for a comparison of these methods. RFM is routinely used in the solar line formation work, as the velocities involved are small. However CMF holds the advantage even in this case, because one can work with angle averaged PRD functions. In the high velocity flows encountered in stellar atmospheres, CMF techniques are always preferred over the RFM. Jeffery (1989, 1990 - 'Sobolev-P' method) and Hillier (1996 - ALI-based CMF method) solved the problem of polarized line formation in spherical/ non-spherical winds. Nagendra (1996) presented a CMF approach for polarized resonance scattering with PRD in planar media, and using the DSM. The relevant CMF transfer equation is

$$\mu \frac{\partial \boldsymbol{\mathcal{I}}(z,x,\mu)}{\partial z} - \left[\mu^2 \frac{dln\ v(z)}{dln\ z}\right] \frac{\partial \boldsymbol{\mathcal{I}}(z,x,\mu)}{\partial x} =$$

$$k^L(z)\ [(\phi(z,x) + \beta(z)]\ \ [-\boldsymbol{\mathcal{I}}(z,x,\mu) + \boldsymbol{\mathcal{S}}(z,x,\mu)], \qquad (12)$$

where $v(r)$ is the velocity of the medium along the symmetry axis, expressed in mean thermal units (1 mtu $= v_{th} = \sqrt{2kT/M_a}$). The approximations involved in formulating the above initio-boundary value problem are described in Mihalas

(1978). Two main steps involved are: (i) computing $\boldsymbol{\mathcal{S}}(z, x, \mu)$ at all the $z-$ points, by solving the above equation in CMF; (ii) performing a Formal Solution (FS) in the observer's frame to obtain $(\mathrm{I\ Q})^{\mathrm{T}}$ along several lines of sight (LOS).

Model parameters used in computing Fig. (2b) are: $[T^L, a, \varepsilon, \beta, B(\tau)] = [100, 10^{-3}, 10^{-4}, 0, 1]$. The PRD function employed is $R_{\mathrm{II-AA}}(x, x')$. A self-emitting slab expanding with a constant velocity of $v(\tau) = 1$ mtu is used. Solid line represents LOS at extreme limb ($\mu = 10^{-3}$) and dashed line the disk center. Progressive limb brightening of emission line profile is seen in the I and Q profiles. The degree of polarization (Q/I) reaches maxima at all frequencies, as one approaches the limb. Blue shift and large distortion cause strong changes in the polarized flux profiles observed from expanding stellar atmospheres. Details of the computation and other parameters are given in Nagendra (1996).

The following conclusions can be drawn from Fig. (2b): (1) CMF method is a preferred technique because a smaller number of N_μ and N_ν, is sufficient when compared to those necessary for RFM computations; (2) the main advantage of CMF method is that we can work with angle averaged redistribution functions, unlike the RFM which require angle dependent redistribution functions. (3) PRD effects on polarization are enhanced by macroscopic velocity fields, due to direct effect of velocity fields on the source function gradient.

5. Polarized Approximate Lambda Iteration (PALI) Methods

We confine our attention to the Hanle scattering line polarization. The resonance scattering polarization is a special case (B = 0) of these equations. We also ignore Zeeman line polarization by true absorption process. There are two parallel streams of development in this field:

Stream-1: Atomic Density Matrix Approach:
Under stream-1, the polarized transfer equation is derived using the 'atomic density matrix theory'. See the formulations in House (1970); Omont, Smith, & Cooper (1973); Landi Degl' Innocenti (1983); Landi Degl' Innocenti, Bommier, & Sahal-Brechot (1990); Bommier (1997); and Bommier, & Stenflo (1999). Solution of RTE for radiation density matrix elements by PALI approach, and solar applications are presented in Trujillo Bueno & Landi Degl' Innocenti (1996, 1997), Trujillo Bueno & Manso Sainz (1999), Manso Sainz & Trujillo Bueno (1999, 2001). CRD mechanism is used in these computations. For a review on older methods of solving the LTE and NLTE polarized transfer equation, see Rees (1987), Rees & Murphy (1987), and Stenflo (1994).

Stream-2: Scattering Phase Matrix Approach:
Under stream-2, the transfer equation is derived using conventional 2-level atom NLTE (Mihalas 1978), or the so called 'scattering approach' (Frisch, 1999). The polarized integral equations are derived in Stenflo & Stenholm (1976), Rees (1978), and Ivanov et al. (1997). These authors consider only CRD to represent polarized line scattering. The solution of transfer equation by PALI approach is presented in Faurobert et al. (1997: PALI-1), Paletou & Faurobert (1997: PALI-2), Nagendra et al. (1998: PALI-3), Nagendra et al. (1999: PALI-4), Nagendra et al. (2000: PALI-5), and Fluri et al. (2002: PALI-6), and other

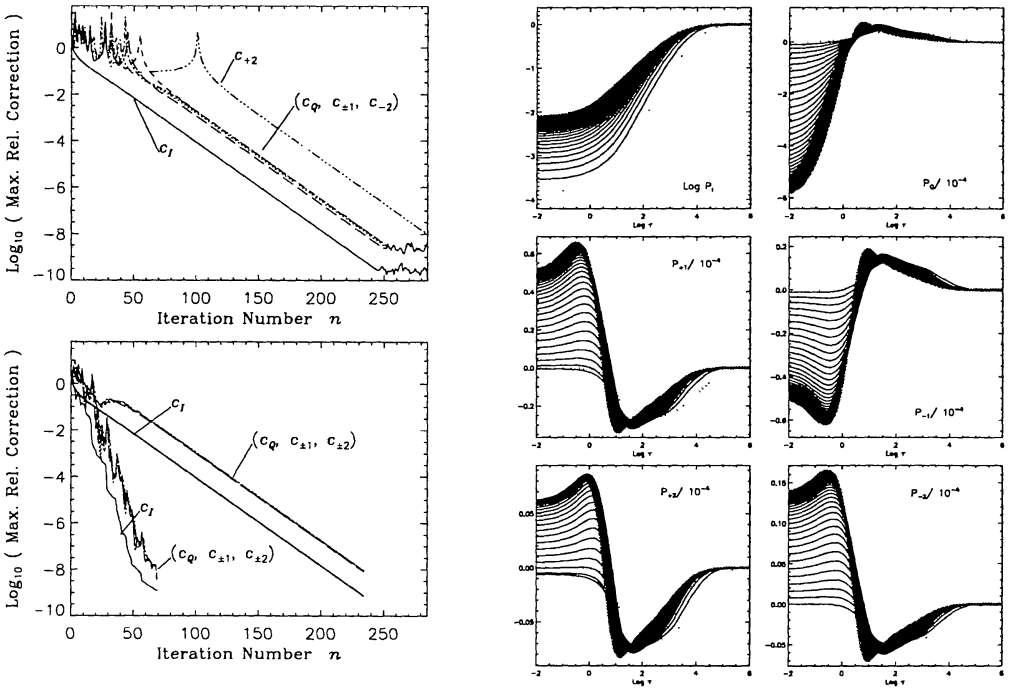

Figure 3. (**a**: Left) Iterative corrections on reduced source vector components in Hanle-CRD problem. (**b**: Right) Convergence characteristics of reduced source vector components in Hanle-PRD problem.

papers connected with this series. Both CRD as well as PRD are considered. Other papers discussing the PALI method under Stream-2 are by Dittman (1999) where CRD in line scattering is considered.

5.1. PALI Method for the Non-axisymmetric Hanle Effect with CRD

Hanle effect is a weak magnetic field effect on atoms. For UV, optical and near infra-red lines, the condition $\Delta\nu_B >> \Gamma_R$ is satisfied when the field strength B $\geq$ 1000 G, where $\Delta\nu_B$ is the Larmour frequency, and Γ_R the radiative width of excited state. In this case, the V-Stokes parameter is coupled to I, Q and U-Stokes parameters, and hence one has to solve the transfer equation for $(\mathrm{I\ Q\ U\ V})^{\mathrm{T}}$. Same condition prevails for B = 300 G − 1000 G (Hanle-Zeeman regime where $\Delta\nu_B > \Gamma_R$ is satisfied). For weak fields (B = 10 G − 100 G) the condition $\Delta\nu_B \leq \Gamma_R$ is satisfied, and represents the case of pure Hanle scattering. The Hanle effect 'modifies' linear polarization produced in a non-magnetic resonance scattering event. In this case Stokes-V is decoupled from $(\mathrm{I\ Q\ U})^{\mathrm{T}}$. Finally B = 0 G corresponds to resonance scattering polarization, and the radiation field can be represented by $(\mathrm{I\ Q})^{\mathrm{T}}$ (axi-symmetry). Unequal population of 'degenerate' magnetic sub-states (caused by angularly anisotropic incidence of radiation on the radiating atom), is responsible for this phenomena.

The geometry of the problem is shown in Nagendra et al. (1998). The 1-D Hanle transfer equation for the Stokes vector $\mathcal{I} = (\mathrm{I\ Q\ U})^{\mathrm{T}}$ has the same form as Eq. (1). Similarly, Eq. (2) and Eq. (3) also hold good, with the new definition

that $\boldsymbol{\mathcal{S}} = (S_{\rm I}\ S_{\rm Q}\ S_{\rm U})^{\rm T}$; and $\boldsymbol{\mathcal{U}} = (1\ 0\ 0)^{\rm T}$. Further, the Rayleigh phase matrix in Eq. (3) has to be replaced by the (3×3) Hanle phase matrix $\hat{P}_{\rm H}(\mathbf{n}, \mathbf{n}', \mathbf{B})$ that depends on magnetic field $\mathbf{B}(\theta_{\rm B}, \varphi_{\rm B}, {\rm B})$. $\boldsymbol{\mathcal{I}}$ and $\boldsymbol{\mathcal{S}}_l$ now depend on azimuthal angle φ. However, one can change this non-axisymmetric transfer problem to a φ independent form by working in 'Fourier space'. It involves an expansion of $\boldsymbol{\mathcal{I}}$ and $\boldsymbol{\mathcal{S}}_l$ in a Fourier series w.r.t φ. We mention only few equations. Full details of the problem are presented in Nagendra et al. (1998).

Fourier Expansion of the Azimuthal Dependence:
The Hanle source vector can be Fourier expanded as:

$$\boldsymbol{\mathcal{S}}(\tau, x, \mu, \varphi) = \overline{S}_0(\tau, x, \mu) + \sum_{k=1}^{k=2} [\overline{S}_k(\tau, x, \mu) \cos k\varphi + \overline{S}_{-k}(\tau, x, \mu) \sin k\varphi], \quad (13)$$

where $\overline{S}_k$ are 3- component vectors. $\overline{S}_0$ has 2- components (by symmetry). An exactly similar expansion holds for intensity vector also. A double Fourier expansion w.r.t φ and φ' is needed for the Hanle phase matrix.

An Additional Factorization:
Defining a 14- component 'Fourier source vector' $S_{\rm F} = \left[\overline{S}_0, \overline{S}_1, \overline{S}_{-1}, \overline{S}_2, \overline{S}_{-2}\right]^{\rm T}$, one can achieve an 'angle and frequency factorization' $S_{\rm F}(\tau, x, \mu) = \hat{B}(\mu) * \mathbf{S}(\tau, x)$, where $\mathbf{S}(\tau, x)$ is a 6- component 'reduced source vector'. First component of $\mathbf{S}(\tau, x)$ is simply the scalar source function $S(\tau, x)$ of unpolarized RTE. The reduced source vector satisfies a vectorial integral equation

$$\mathbf{S}(\tau, x) = (1-\varepsilon)\hat{H}_{\rm B}(\theta_{\rm B}, \varphi_{\rm B}, {\rm B}) \int_0^T \hat{K}(x, \tau - \tau')\mathbf{S}(\tau', x)\, d\tau' + \varepsilon B_{\nu_o}(\tau)\mathbf{U}. \quad (14)$$

The kernel matrix K is independent of magnetic field, and is written as

$$\hat{K}(x, \tau) = \begin{pmatrix} K_{11} & K_{12} & 0 & 0 & 0 & 0 \\ K_{12} & K_{22} & 0 & 0 & 0 & 0 \\ 0 & 0 & K_{33} & 0 & 0 & 0 \\ 0 & 0 & 0 & K_{33} & 0 & 0 \\ 0 & 0 & 0 & 0 & K_{44} & 0 \\ 0 & 0 & 0 & 0 & 0 & K_{44} \end{pmatrix}. \quad (15)$$

$\hat{H}_{\rm B}$ is (6×6) magnetic matrix (Nagendra 1998). Note that $\hat{H}_{\rm B} = \hat{I}$, when ${\rm B} = 0$.

$$\hat{H}_{\rm B}(\theta_{\rm B}, \varphi_{\rm B}, {\rm B}) = \hat{R}(\varphi_{\rm B})\ \hat{M}_{\rm B}(\theta_{\rm B}, {\rm B})\ \hat{R}(-\varphi_{\rm B}), \quad (16)$$

where $\hat{R}(\varphi_{\rm B})$ is the rotation matrix ($\hat{R}(0) = \hat{I}$), with $\hat{I}$ being a unit matrix.

The Reduced Hanle Transfer Equation in Fourier Space:
The 'axi-symmetric' RTE for 6-component reduced intensity vector $\mathbf{I}(\tau, x, \mu)$ is

$$\mu \frac{\partial \mathbf{I}(\tau, x, \mu)}{\partial \tau} = (\phi(\tau, x) + \beta(\tau))\ [\mathbf{I}(\tau, x, \mu) - \mathbf{S}(\tau, x)]. \quad (17)$$

Notice that $\mathbf{I}$ does not depend on φ. And $\mathbf{S}$ neither depends on φ nor on μ. The total reduced source vector is

$$\mathbf{S}(\tau,x) = \frac{\phi(\tau,x)\ \mathbf{S}_l(\tau,x)\ +\ \beta(\tau)B_{\nu_o}(\tau)\mathbf{U}}{\phi(\tau,x)+\beta(\tau)}, \qquad \mathbf{U} = (1\ 0\ 0\ 0\ 0\ 0)^{\mathrm{T}}, \tag{18}$$

where the reduced line source vector may be written as

$$\mathbf{S}_l(\tau,x) = (1-\varepsilon)\ \hat{H}_{\mathrm{B}}(\theta_{\mathrm{B}},\varphi_{\mathrm{B}},\mathrm{B})\ \mathbf{J}(\tau,x)\ +\ \varepsilon B_{\nu_o}(\tau)\mathbf{U}\ . \tag{19}$$

The scattering integral $\mathbf{J}$ is given by,

$$\mathbf{J}(\tau,x) = \frac{1}{2}\int_{-\infty}^{+\infty}\ \int_{-1}^{+1}\ \frac{R(\tau,x,x')}{\phi(\tau,x)}\ \hat{B}^{\mathrm{T}}(\mu')\hat{B}(\mu')\,\mathbf{I}(\tau,x',\mu')\,d\mu'\,dx'. \tag{20}$$

Expressions for the (14×6) matrix $\hat{B}(\mu)$ are given in Nagendra et al. (1998). We now present PALI method for Hanle effect with CRD, namely $R(x,x') = \phi(x)\ \phi(x')$. The CRD source functions are independent of x, but this dependence is kept in the equations, in view of applicability in PRD case (Sect. 5.2).

PALI *Numerical Method of Solution for Hanle Effect with* CRD*:*
We give below a few important equations only. At any depth point τ_i the reduced source vector satisfies the integral equation

$$\mathbf{S}(\tau_i)\ =\ (1-\varepsilon)\ \hat{H}_{\mathrm{B}}\ \hat{\Lambda}_{ii}\ [\mathbf{S}(\tau_i)]\ +\ \varepsilon B_{\nu_0}(\tau_i)\mathbf{U}. \tag{21}$$

The reduced mean intensity for the CRD case is

$$\mathbf{J}(\tau_i) = \hat{\Lambda}_{ii}\ [\mathbf{S}(\tau_i)] = \int_{-\infty}^{+\infty}\phi(\tau_i,x')dx'\ \frac{1}{2}\int_{-1}^{+1}\hat{B}^{\mathrm{T}}(\mu')\hat{B}(\mu')\ \mathbf{I}(\tau_i,x',\mu')d\mu'. \tag{22}$$

The source vector corrections at the nth iteration are computed using

$$\delta\mathbf{S}^{(n)}(\tau_i) = \left[\hat{L}^*(\tau_i)\right]^{-1}\ \left[\varepsilon B_{\nu_0}(\tau_i)\mathbf{U} - \left\{\mathbf{S}^{(n)}(\tau_i) - (1-\varepsilon)\hat{H}_{\mathrm{B}}\ \mathbf{J}^{(n)}(\tau_i)\right\}\right], \tag{23}$$

where $\mathbf{S}^{(n)}(\tau_i)$ is the current estimate, and the mean intensity $\mathbf{J}^{(n)}(\tau_i)$ must explicitly be computed using a formal solver FS. The frequency independent (CRD) approximate lambda operator $\hat{L}^*$ is a $(6N_d\times 6N_d)$ global 'block diagonal operator' with one (6×6) block at every depth i. Such a block is written as

$$\hat{L}^*(\tau_i)\ =\ \left[\mathbf{E}\ -\ (1-\varepsilon)\,\hat{H}_{\mathrm{B}}\ ,\hat{\Lambda}^*\right]. \tag{24}$$

The maximum relative corrections are $c_\alpha^{(n)}$, where $\alpha = \mathrm{I},\ \mathrm{Q},\ \pm 1,\ \pm 2$ refer to components of the source vector. The quantity $\mathbf{E}$ is a (6×6) identity operator. Stokes source vector can be obtained from the reduced source vector by simple transformation [see Eqs. (24)-(26) in Frisch (1999)]. Same transformation holds for intensity vectors also with source terms replaced by intensity terms.

The Discussion on Fig. (3a) *and Conclusions:*
To compute the results presented in Fig. (3a), a two -level atom model, and an isothermal, self-emitting, symmetric slab with the parameters $[T, a, \varepsilon, \beta, B_\nu] = [2 \times 10^9,\ 10^{-3},\ 10^{-6},\ 0,\ 1]$ is employed. The magnetic field parameters are $[\Gamma_{\rm B},\ \theta_{\rm B},\ \varphi_{\rm B}] = [1,\ 30^\circ,\ 0^\circ]$. The iterative convergence is controlled by the I component. The other 5 modes of the reduced intensity remain as subsidiaries. The convergence rate of PALI method is independent of $\mathbf{B}$. The spike in c_{+2} during a stable phase is caused by zero crossing of polarized source components. When zero-crossing point in optical depth space coincides with a spatial grid point, the conventional definition of MRC undergoes artificial spikes, showing that it is not a reliable measure of iterative convergence. The lower panel shows the smooth convergence behaviour when a 'modified definition' of MRC (Nagendra 1998) is used. The usefulness of Ng acceleration is also shown in this panel. Note that all curves have asymptotically same slope for large values of n. In practical work, a simple test based on the convergence of surface polarization is good enough.

5.2. PALI Method for the Non-axisymmetric Hanle Effect with PRD

We generalize core-wing method of Paletou & Auer (1995) to include polarization of line radiation. Only few equations are given below to highlight the nature of this method. See Nagendra et al. (1999) for more details of PALI method for Hanle effect with PRD. Eqs. (13)-(20) of Sect. 5.1 hold good in the PRD case also.

PALI *Numerical Method of Solution for Hanle Effect with* PRD*:*
The iterative corrections to the reduced source vector are given by the expression

$$\delta\mathbf{S}_{l,x}^{(n)} - (1-\varepsilon)\ \hat{H}_{\rm B} \int_{-\infty}^{+\infty} g_{x,x'}\ p_{x'}\ \hat{L}_{x'}^{*}[\delta\mathbf{S}_{l,x'}^{(n)}]\ dx' \ = \ \mathbf{r}_x^{(n)}, \qquad (25)$$

where $g_{x,x'} = R_{x,x'}/\phi_x$ are PRD redistribution weights and $p_x = \phi_x/(\phi_x + \beta)$. The total corrections are $\delta\mathbf{S}_x^{(n)} = p_x \delta\mathbf{S}_{l,x}^{(n)}$. The monochromatic (PRD) approximate operator $\hat{L}_x^*$ represents diagonal part of full operator $\hat{L}_x$ (i.e we employ a block-Jacobi method). The operator splitting $\hat{L}_x = \hat{L}_x^* + (\hat{L}_x - \hat{L}_x^*)$ allows to make this choice. It is pre-computed and stored as a block-diagonal matrix of dimension $(6N_dN_x \times 6N_dN_x)$ (hence requires considerable computing time). The residual function $\mathbf{r}_x^{(n)}$ is given by

$$\mathbf{r}_x^{(n)} \ = \ (1-\varepsilon)\ \hat{H}_{\rm B}\ \mathbf{J}_x^{(n)} \ - \ \mathbf{S}_{l,x}^{(n)} \ + \ \varepsilon B_{\nu_o}\mathbf{U}; \quad \text{where} \quad \mathbf{U} = (1\ 0\ 0\ 0\ 0\ 0)^{\rm T}. \qquad (26)$$

Meaning of the core-wing Approximation for Line Scattering:
The weighted separation of frequency integral over a given function $\mathbf{f}_x$ as

$$\int_{-\infty}^{+\infty} g_{x,x'}\mathbf{f}_{x'}\,dx' \approx (1-\alpha_x)\int_{core} \phi_{x'}\mathbf{f}_{x'}\,dx' + \alpha_x \int_{wing} \delta(x-x')\mathbf{f}_{x'}\,dx', \qquad (27)$$

is called the core-wing procedure. The separation coefficient $\alpha_x = 0$ for $x < x_c$ (line core), and $\alpha_x = \mathrm{diag}\{g_{i,j}\},\ i,j = 1, N_x,$ for $x > x_c$ (line wing). We assume

that the core-wing cut-off frequency $x_c = 3.5$. The core and wing corrections can be calculated separately as follows.

Corrections in the Core Domain ($x < x_c$):

$$\delta \mathbf{S}_{l,x}^{(n)} = \hat{H}_{\rm B}\ \mathbf{\Delta T}^{(n)} + \mathbf{r}_x^{(n)}, \tag{28}$$

where the 'frequency independent' operator $\mathbf{\Delta T}^{(n)}$ is computed by

$$\left[\hat{I} - (1-\varepsilon)\ \hat{H}_{\rm B}\ \overline{\hat{L}}^{\,*}\right] \mathbf{\Delta T}^{(n)} = \overline{\mathbf{r}}^{(n)}, \tag{29}$$

with the frequency averaged operator $\overline{\hat{L}}^{\,*}[\ ]$ and $\overline{\mathbf{r}}^{(n)}$ given by

$$\overline{\hat{L}}^{\,*}[\ ] = \int_{core} \phi_{x'}\ p_{x'}\ \hat{L}^*_{x'}[\ ]\ dx', \tag{30}$$

$$\overline{\mathbf{r}}^{(n)} = (1-\varepsilon) \int_{core} \phi_{x'}\ p_{x'}\ \hat{L}^*_{x'}[\mathbf{r}^{(n)}_{x'}]\ dx'. \tag{31}$$

Corrections in the Wing Domain ($x > x_c$):

$$\left[\hat{I} - \alpha_x(1-\varepsilon)\ \hat{H}_{\rm B}\ p_x\ \hat{L}^*_x\right]\ \delta \mathbf{S}_{l,x}^{(n)} = \mathbf{r}_x^{(n)} + (1-\alpha_x)\ \hat{H}_{\rm B}\ \mathbf{\Delta T}^{(n)}. \tag{32}$$

The formal solution (FS) is calculated by a short characteristics method. Eqs. (28), (29), and (32) are main equations of the core-wing method.

Convergence Characteristics of core-wing PALI *Method:*
Convergence tests are similar to that of Hanle/CRD problem. The 'convergence rate' is independent of the magnetic field. On the Hanle/PRD problem, PALI is about 80 times faster than perturbative Feautrier method (scalar Feautrier + polarization by perturbation). PALI requires 30 times less memory than Feautrier perturbative method. Scaling is: Feautrier method [CPU time $\sim N_t^3$, memory $\sim N_t^2$], and PALI method [CPU time $\sim N_t$, memory $\sim N_t$], where $N_t = N_\nu * N_\mu$.

The Discussion on Fig. (3b) *and Conclusions:*
The history of convergence of six source vector components $\mathbf{P}(\tau, x) = \mathbf{J}(\tau, x) + \varepsilon B_{\nu_0}\mathbf{U}$ at $x = 0$ is shown in Fig. (3b). $\mathbf{P}(\tau, x)$ is plotted as a function of τ upto mid-slab. Last 5 polarized components are divided by 10^{-4} for convenience. An isothermal, self-emitting, symmetric slab model with parameters $[T, a, \varepsilon, \beta, B_{\nu_0}] = [2 \times 10^6, 10^{-3}, 10^{-4}, 0, 1]$ is employed. Magnetic field parameters are $[\Gamma_{\rm B}, \theta_{\rm B}, \varphi_{\rm B}] = [1, 30^\circ, 0^\circ]$. The dotted line represents the solution on the first iteration. The last 4 harmonic modes (± 1 and ± 2) are smaller in magnitude, and guided by the Q - component, which in turn, is a slave mode of the dominant I - component. Notice a perfectly uniform convergence of PALI iterations.

6. Conclusions and an Overview

(1) Direct methods have a role to play in the polarized line transfer theory by providing accurate bench-marks (a) to check correctness and accuracy of

modern PALI codes; (b) to explore new physical effects, as direct methods like Feautrier method or DSM, are relatively easy to generalize to the polarized case (see e.g., Nagendra, & Peraiah 1985; Poutanen, Nagendra, & Svensson 1996), unlike iterative methods. **(2)** PALI and its variants are the methods of choice for analyzing polarimetric data, and stellar atmospheric modeling, due to smaller requirements of memory and CPU time. **(3)** The word approximate in the so called "approximate methods", refers only to the choice of the local lambda operator, and not to the solution, which indeed remains as accurate as that from a direct method, and contains much less round-off errors.

Some interesting problems of polarized line transfer which require attention in the near future are: (1) combined Zeeman-Hanle PRD problem in intermediate fields (300 G $\leq B \leq$ 1000 G); (2) Hanle-PRD in multi-D geometry for solar and stellar applications; (3) Hanle-PRD with multi-level atomic coupling in order to model the observed data. High resolution solar polarimetric observations can distinguish relative contribution of such effects.

References

Bommier, V. 1997, A&A, 328, 726

Bommier, V., & Sahal-Brechot, S. 1978, A&A, 69, 57

Bommier, V., & Stenflo, J.O. 1999, A&A, 350, 327

Chandrasekhar, S. 1950. Radiative Transfer (Oxford: Clarendon Press)

Dittman, O.J. 1999, in Solar Polarization ed. K.N. Nagendra & J.O. Stenflo, ASSL 243 (Dordrecht: Kluwer), 201

Dumont, S., Omont, A., Pecker, J.C., & Rees, D.E. 1977, A&A, 54, 675

Faurobert, M. 1987, A&A, 178, 269

Faurobert, M., Frisch, H., & Nagendra, K.N. 1997, A&A, 322, 896 (**PALI-1**)

Fluri, D.M., Nagendra, K.N., & Frisch, H. 2002, A&A, (Accepted) (**PALI-6**)

Frisch, H. 1998, A&A, 338, 683

Frisch, H. 1999, in Solar Polarization, ed. K.N. Nagendra & J.O. Stenflo, ASSL 243 (Dordrecht: Kluwer), 97

Grant, I.P. & Hunt, G.E. 1969a, Proc. Roy. Soc. Lond., A 313, 183

Grant, I.P. & Hunt, G.E. 1969b, Proc. Roy. Soc. Lond., A 313, 199

Hamilton, D.R. 1947. ApJ, 105, 424

Heinzel, P. 1981, JQSRT 25, 483

Hillier, D.J. 1996, A&A, 308, 521

House, L. 1970, JQSRT, 10, 1171

Hubeny, I. 1985, in Progress in Stellar Spectral Line Formation Theory, ed: J.E. Beckman & L. Crivellari, NATO ASI Ser. C.152, (Dordrecht: Reidel)

Hubeny, I. 1992, in The Atmospheres of Early-Type Stars, Lecture Notes in Phys. 401, ed. U. Heber, & C.J. Jeffery (Berlin: Springer), 377

Hummer, D.G. 1962, MNRAS, 125, 1

Ivanov, V.V. 1991, in Stellar Atmospheres: Beyond Classical Models, ed. L. Crivellari, I. Hubeny, & D.G. Hummer NATO ASI Series C341 (Dordrecht: Reidel), 81

Ivanov, V.V., Grachev, S.I., & Loskutov, V.M. 1997, A&A, 321, 968

Jeffery, D.J. 1989, ApJS, 71, 951

Jeffery, D.J. 1990, ApJ, 352, 267

Landi Degl' Innocenti, E. 1982, Sol. Phys., 79, 291

Landi Degl' Innocenti, E. 1983, Sol. Phys., 85, 3

Landi Degl' Innocenti, E. 1984, Sol. Phys., 91, 1

Landi Degl' Innocenti, E. 1985, Sol. Phys., 102, 1

Landi Degl' Innocenti, E., Bommier, V., & Sahal-Brechot, S. 1990, A&A, 235, 459

Manso Sainz, M., & Trujillo Bueno, J. 1999, in Solar Polarization, ed. K.N. Nagendra & J.O. Stenflo, ASSL 243 (Dordrecht: Kluwer), 143

Manso Sainz, M., & Trujillo Bueno, J. 2001, in ASP Conf. Ser. Vol. 236, Advanced Solar Polarimetry - Theory, Observations, & Instrumentation, ed. M. Sigwarth, (San Francisco: ASP), 213

Mc Kenna, S.J. 1984, Ap&SS, 106, 283

Mihalas, D. 1978, Stellar Atmospheres (San Francisco: Freeman)

Nagendra, K.N., & Peraiah. 1985, MNRAS, 214, 203

Nagendra, K.N. 1986, PhD Thesis (Bangalore: Bangalore Univ.)

Nagendra, K.N. 1988, ApJ, 335, 269

Nagendra, K.N. 1994, ApJ, 432, 274

Nagendra, K.N. 1995, MNRAS, 274, 523

Nagendra, K.N. 1996, Sol. Phys., 164, 67

Nagendra, K.N., Frisch, H., & Faurobert, M. 1998, A&A, 332, 610 (**PALI-3**)

Nagendra, K.N., Frisch, H., Faurobert, M., & Paletou, F. 2000, JAA, 21, 255 (**PALI-5**)

Nagendra, K.N., Paletou, F., Frisch, H., & Faurobert, M. 1999, ed. K.N. Nagendra & J.O. Stenflo, ASSL 243 (Kluwer: Dordrecht), 127 (**PALI-4**)

Olson, G.L., Auer, L.H., & Buchler, J.R. 1986, JQSRT, 35, 431

Omont, A., Smith, E.W., & Cooper, J. 1973, ApJ, 182, 283

Paletou, F., & Auer, L.H. 1995, 297, 771

Paletou, F, & Faurobert, M. 1997, A&A, 328, 343 (**PALI-2**)

Peraiah, A. 2001, An Introduction to Radiative Transfer, (Cambridge: CUP)

Poutanen, J., Nagendra, K.N., & Svensson, R. 1995, MNRAS, 283, 892

Redheffer, R. 1962, J. Math. Phys., 41, 1

Rees, D.E. 1978, PASJ, 30, 455

Rees, D.E. 1987, in Numerical Radiative Transfer, ed. W. Kalkofen (Cambridge: CUP), 213

Rees, D.E., & Murphy, G.A. 1987, in Numerical Radiative Transfer, ed. W. Kalkofen (Cambridge: CUP), 241

Rees, D.E., & Saliba, G.J. 1982, A&A, 115, 1

Stenflo, J.O., & Stenholm, L.G. 1976, A&A, 46, 69

Stenflo, J.O. 1994, Solar Magnetic Fields: Polarized Radiation Diagnostics (Dordrecht: Kluwer)

Trujillo Bueno, J., & Landi Degl' Innocenti, E. 1996, Sol. Phys., 164, 135

Trujillo Bueno, J., & Landi Degl' Innocenti, E. 1997, ApJL, 482, 183

Trujillo Bueno, J., & Manso Sainz, R. 1999, ApJ, 516, 463